A Comparative Study of Different Phase Detrending Algorithms for Scintillation Monitoring

URSI GASS 2020, Rome, Italy, 29 August - 5 September 2020

A Comparative Study of Different Phase Detrending Algorithms for Scintillation Monitoring

Hossein Ghobadi*[(1)(2)], Caner Savas[(3)], Luca Spogli[(1)(4)], Fabio Dovis[(3)], Antonio Cicone[(5)], and Massimo Cafaro[(2)]
(1) Istituto Nazionale di Geofisica e Vulcanologia, Rome, Italy
(2) Department of Engineering for Innovation, University of Salento, Lecce, Italy
(3) Department of Electronics and Telecommunications, Politecnico di Torino, Turin, Italy
(4) SpacEarth Technology, Rome, Italy
(5) University of Insubria, Como, Italy

Abstract

Rapid and sudden fluctuations of phase and amplitude in Global Navigation Satellite System (GNSS) signals due to diffraction of the ionosphere phase components when signals passing through small-scale irregularities (less than hundreds meters) are commonly so-called ionospheric scintillation. The aim of the paper is to analyze the implementation and compare the performance of different phase detrending algorithms to improve scintillation monitoring. Three different phase detrending methods, namely, three cascaded second-order high pass filters, six order Butterworth filter conducted by cascading six first-order high pass Butterworth filters, and Fast Iterative Filter (FIF) are considered in this paper. The study exploits real GNSS signals (GPS L1, Galileo E1b) affected by significant phase scintillation effects, collected in early September 2017 at Brazilian Centro de Radioastronomia e Astrofisica Mackenzie (CRAAM) monitoring station and at Adventdalen (Svalbard, Norway) research station. In this study, a software-defined radio (SDR) based GNSS receiver is used to process GNSS signals and to implement the aforementioned detrending algorithms.

1 Introduction

The varied range of irregularities from centimeters up to few hundreds of kilometers in the ambient ionosphere with respect to the plasma drift velocity impose perturbations on Global Navigation Satellite System (GNSS) signals. The nature of the perturbation depends on the typical scale of the irregularities and on their dynamics. The threshold separating small and large scale irregularities is given by the Fresnel's scale. Irregularities having scale sizes above the Fresnel's scale result into refractive effect of the trans-ionospheric signals, because of the variation of the refractive index of the ionosphere. Below the Fresnel's scale, refractive and diffractive effects concur. The latter are due to the fact that, when crossed by the plane-wave, small-scale irregularities act as new wave source, resulting into an interference pattern when received at ground [1].

The ionospheric component of the phase equation can be represented by both a refractive component (deterministic), and a diffractive component (stochastic) [2]. Only the fluctuations due to diffractive effects are termed "scintillations" [2, 3]. In order to quantify and characterize the phase scintillations, phase scintillation indices computed from the phase of the received GNSS signals are used. The necessity for detrending the phase arises from the need of including only the high-frequency fluctuations due to diffraction in the phase scintillation index. Furthermore, precise estimation of the scintillation intensity under the effects of error sources (e.g. thermal noise, oscillator noise, etc.) is important for scintillation monitoring applications, hence the design of the detrending filter gains importance to estimate the scintillation indices.

Generally, most GNSS receivers designed for the purpose of ionospheric scintillation monitoring use designed high pass filters or Butterworth filters with a fixed cutoff frequency of 0.1 Hz to remove low frequency trends from the data [4]. Moreover, filtering techniques such as cascaded high pass filters and Butterworth filters are based on classical time-frequency analysis where they need *a priori* assumptions, and uncertainty principle is another obstacle. However new filtering techniques such as Ensembled Empirical Mode Decomposition (EEMD) and those implementing the iterative filtering (like the Adaptive Local Iterative Filtering (ALIF) [5] and the Fast Iterative Filtering (FIF) [6]) do not deal with these issues.

In this study, leveraging on the capability of three different detrending approaches, namely, three cascaded second-order high pass filters, six order Butterworth filter conducted by cascading six first-order high pass Butterworth filters, and Fast Iterative Filter (FIF), we analyze scintillation events through collected real GNSS signals (GPS L1 and Galileo E1b) for several satellites affected by significant phase scintillation effects. We select FIF, because (1) IF-family techniques have been proven to overperform EEMD for the time-frequency analysis of a non-stationary signal [7] and (2) FIF convergence and stability have been mathematically proven [6].

We exploit the datasets collected in early September 2017 at Brazilian Centro de Radioastronomia e Astrofisica

Mackenzie (CRAAM) monitoring station and at Adventdalen (Svalbard, Norway) research station. Although inherent characteristics of the ionospheric effect at different regions require different detrending settings, the standard cut-off frequency 0.1 Hz is set for the phase detrending in this paper. We are aware that such choice is not suitable for high-latitude data [2, 8] but the purpose of this work is the comparison of the filtering methods and not to optimize the cutoff selection.

The paper is organized as follows. In Section 2, we introduce the phase detrending methods. In Section 3, performance analysis of the methods are discussed. Finally, Section 4 draws conclusion.

2 Phase Detrending Methods

Phase scintillation monitoring is achieved by computing the σ_ϕ index that corresponds to the standard deviation of the detrended phase measurements [9]:

$$\sigma_\phi = \sqrt{\langle \varphi^2 \rangle_T - \langle \varphi \rangle_T^2}, \tag{1}$$

where φ is the detrended phase measurement that can be obtained by processing the carrier phase measurements through the filters. $\langle \cdot \rangle_T$ is the average operation over a fixed period T which generally denotes a 1-min average [9].

In the following subsections, the phase detrending methods are summarized.

2.1 Cascaded High Pass Filters

In this phase detrending algorithm, the phase measurements are passed through three cascaded 2^{nd} order high pass filters (HPFs), and all low-frequency effects are removed [10]. The filter form is as shown in Fig. 1.

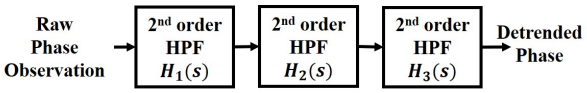

Figure 1. Cascaded HPF design for phase detrending.

Each stage filter has a form in the s-plane [10]:

$$H_i(s) = \frac{s^2}{s^2 + \alpha_i \omega_N s + \omega_N^2} \tag{2}$$

where $f_N = \omega_N/(2\pi)$ is the filter's corner frequency in Hz. α_1, α_2, and α_3 are the coefficients, the product $H_1(s)H_2(s)H_3(s)$ makes up the frequency response of the high-pass filter.

An interested reader can find more information related to the selection of the coefficients and cutoff frequency in [10].

2.2 Butterworth Filter

In another detrending method, described in [4] is based on the use of a Butterworth filter that can be implemented by cascading six 1^{st} order high-pass Butterworth filters, each with a cutoff frequency $f_c^{'}$ as depicted in Fig. 2.

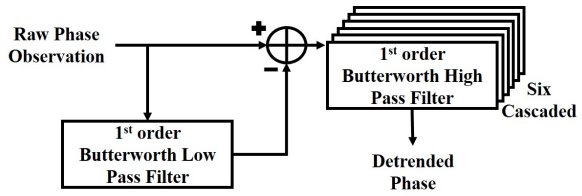

Figure 2. Block diagram of Butterworth filtering for carrier phase data.

The equivalent cutoff frequency cutoff frequency of each filter is computed by [11]:

$$f_c = \frac{f_c^{'}}{\sqrt{2^{1/N} - 1}} \tag{3}$$

where N is set to 6 in our case and setting $f_c = 0.1$ Hz, it is obtained that $f_c^{'} = 0.035$ Hz.

The selection of 0.1 Hz is proposed in [10] and the motivation behind cascading a number of lower-order high-pass Butterworth filters instead of employing one higher-order filter is to overcome the problem of phase shift between input and output [4, 11].

2.3 Fast Iterative Filter (FIF)

FIF is a new detrending technique that is based on the decomposition of a non-stationary nonlinear signal into functions named Intrinsic Mode Components (IMCs), each of them characterized by its frequency v:

$$s = \sum_{i=1}^{N_{IMC}} IMC_i(v) + res. \tag{4}$$

where N_{IMC} is the total number of IMCs and res is the residual that is discarded in our analysis. FIF inherits its algorithmic structure from Empirical Mode Decomposition (EMD) technique but with a stronger mathematical basis that ensures the convergence and stability of the algorithm [6]. Moreover, in [7], a detailed comparison of alternative techniques, namely, Fourier, wavelet, EEMD, and adaptive local iterative filtering (ALIF), for the time-frequency analysis of non-stationary signals is presented.

The cutoff frequency will be set in the equation below:

$$\varphi_{detr}(\Delta t) = \sum_i IMC_i^{v \geq v_c}(\Delta t) \tag{5}$$

where v_c is the cutoff frequency, hence for time interval Δt between t_0 and t_{0+1} minute and detrended phase (φ_{detr}), the value of σ_ϕ will be computed using the phase detrended as in (4).

3 Test Results

Throughout our analysis, a software-defined radio (SDR) based GNSS receiver is used to post-process raw sampled GNSS data and to implement the aforementioned detrending algorithms in the previous section. The datasets collected at Svalbard (78.169°N, 15.993°E) and CRAAM (71.673°S, 2.841°W) monitoring stations are processed and they show different inherent scintillation characteristics due to the different regions.

Fig. 3 and 4 show the computed phase scintillation indices for GPS L1 signals broadcast from satellites PRN-6 and PRN-9 on September 8, 2017, in Svalbard. As it can be noticed starting around 18:40, there is a sharp increase indicating meaningful phase fluctuations.

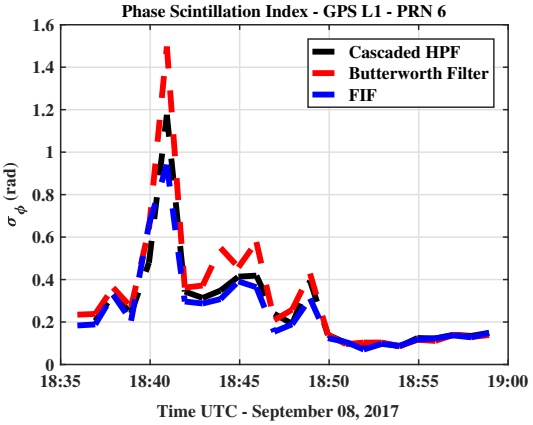

Figure 3. GPS L1 PRN-6 phase scintillation index (σ_ϕ) – September 8, 2017, Svalbard.

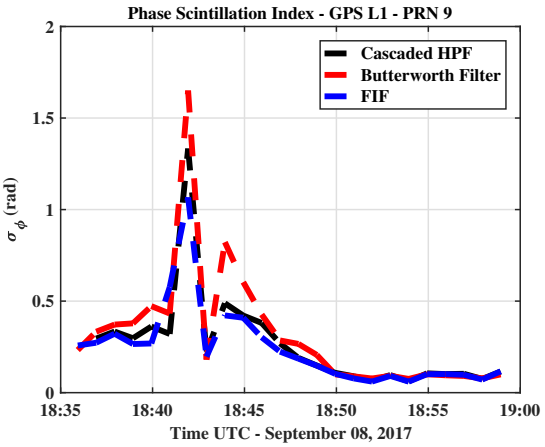

Figure 4. GPS L1 PRN-9 phase scintillation index (σ_ϕ) – September 8, 2017, Svalbard.

As it can be seen in Fig. 5 and 6, at the same time on September 8, 2017, the computed scintillation indices for Galileo E1 signals broadcast from satellites PRN-4 and PRN-19 indicate the event featured by meaningful phase fluctuations as well. For both GPS and Galileo signals, it is observed the computed σ_ϕ follows the same trend in all detrending methods, and FIF could be evaluated as a reliable technique.

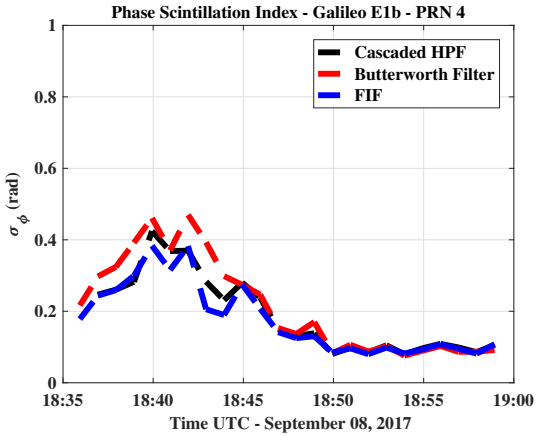

Figure 5. Galileo E1 PRN-4 phase scintillation index (σ_ϕ) – September 8, 2017, Svalbard.

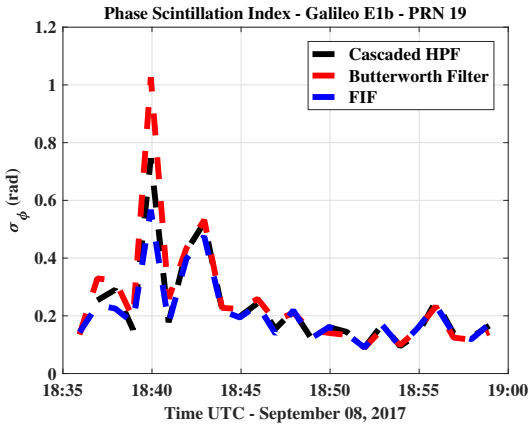

Figure 6. Galileo E1 PRN-19 phase scintillation index (σ_ϕ) – September 8, 2017, Svalbard.

After having compared the performances of different detrending methods under the event that occurred in high latitude region, we also analyze the dataset collected in Brazil. However, it has to be noted that no relevant amplitude scintillation is detected in agreement with the typical behavior of the polar ionosphere in Svalbard [12]. Furthermore, in the datasets collected at the CRAAM monitoring station, it is observed that phase scintillation is accompanied by amplitude scintillation.

Fig. 7 shows the computed phase scintillation indices for the dataset collected on September 13, 2017, at the Brazilian CRAAM monitoring station. It indicates that phase scintillation occurred starting from 02:15 as denoted by the sharp increases in the indices. By processing raw sampled GPS L1 signals that are broadcast from PRN-10 satellite experiencing strong and moderate phase scintillation, the performance of the detrending methods is compared. As

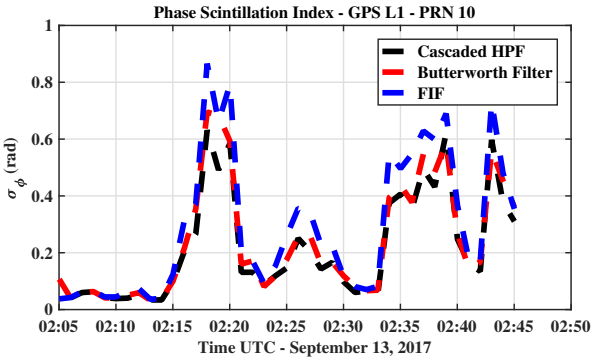

Figure 7. GPS L1 PRN-10 phase scintillation index (σ_ϕ) – September 13, 2017, Brazil.

it can be seen, the results are in parallel with the ones observed in the first dataset.

4 Summary and Conclusions

This work is a comparative study on different phase detrending techniques for ionospheric scintillation events in high and low latitudes in September 2017. Two filtering techniques, namely, three cascaded second-order high pass filters and six order Butterworth filter conducted by cascading six first-order high pass Butterworth filters for scintillation analysis compared to a new filtering technique so-called FIF. The experiments show that FIF is a reliable detrending technique for the ionospheric phase scintillation estimation. The technique performs better if the preprocessing step is manipulated adequately and the cutoff frequency is set efficiently. Therefore an adaptive method shall be developed to adapt the technique to widespread data and to increase the FIF's performance. This open discussion may handle ionospheric scintillation monitoring service to a real-time approach.

5 Acknowledgments

This research work is undertaken under the framework of the TREASURE project (Grant Agreement N. 722023) funded by European Union's Horizon 2020 Research and Innovation Programme within Marie Skłodowska-Curie Actions Innovative Training Network.

Moreover, we would like to thank Alex Minetto for providing the collected datasets in Svalbard, Norway. We also wish to thank Dr. Giorgiana De Franceschi, Dr. Lucilla Alfonsi, Dr. Vincenzo Romano, and Dr. Claudio Cesaroni for the useful discussions supporting the work.

References

[1] Wernik, A. W., Secan, J. A., and Fremouw, E. J., "Ionospheric irregularities and scintillation," *Advances in Space Research*, Vol. 31, No. 4, 2003, pp. 971–981.

[2] McCaffrey, A. M., and Jayachandran, P. T., "Determination of the refractive contribution to GPS phasescintillation," *Journal of Geophysical Research: Space Physics*, Vol. 124, No. 2, 2019, pp. 1454–1469.

[3] De Franceschi, G., Spogli, L., Alfonsi, L., Romano, V., Cesaroni, C., and Hunstad, I., "The ionospheric irregularities climatology over Svalbard from solar cycle 23," *Sci Rep*, 9, 9232, 2019.

[4] Najmafshar, M., Skone, S., and Ghafoori, F., "GNSS data processing investigations for characterizing ionospheric scintillation," In Proceedings of the ION GNSS+ 2014, Tampa, Florida, September 2014, pp. 1190-1202.

[5] Cicone, A., Liu, J., and Zhou, H., "Adaptive local iterative filtering for signal decomposition and instantaneous frequency analysis," *Applied and Computational Harmonic Analysis*, Vol. 41, No. 2, September 2016, pp. 384–411.

[6] Cicone, A. and Zhou, H. "Numerical analysis for iterative filtering with new efficient implementations based on FFT," *arXiv*, October 2018, arXiv preprint arXiv:1802.01359.

[7] Piersanti, M., Materassi, M., Cicone, A., Spogli, L., Zhou, H., and Ezquer, R. G. "Adaptive local iterative filtering: A promising technique for the analysis of nonstationary signals," *Journal of Geophysical Research: Space Physics*, Vol. 123, No.1, 2018, pp. 1031–1046.

[8] Romano, V., Ghobadi, H., Spogli, L., Cafaro, M., Alfonsi, L., Cicone, A., and Linty, N., "Disentangling ionospheric refraction and diffraction effects in GNSS raw phase through Fast Iterative Filtering technique," In AGU Fall Meeting, December 2019.

[9] Mushini, S. C., Jayachandran, P. T., Langley, R. B., MacDougall, J. W., and Pokhotelov, D., "Improved amplitude- and phase-scintillation indices derived from wavelet detrended high-latitude GPS data," *GPS Solut*, 16, pp. 363–373, 2012.

[10] Van Dierendonck, A. J., Klobuchar, J., and Hua, Q., "Ionospheric scintillation monitoring using commercial single frequency C/A code receivers," In Proceedings of the ION GPS 1993, Salt Lake City, UT, September 1993, pp. 1333–1342.

[11] Ghafoori, F. and S. Skone, "Impact of equatorial ionospheric irregularities on GNSS receivers using real and synthetic scintillation signals," *Radio Sci.*,50, pp. 294–317, 2015.

[12] Linty, N., Minetto, A., Dovis, F., and Spogli, L., "Effects of phase scintillation on the GNSS positioning error during the september 2017 storm at Svalbard," *Space Weather*, 16, September 9, 2018, pp. 1317–1329.